ELSEVIER

Influence of copper ions on the precipitation of goethite and hematite in highly alkaline media

Stjepko Krehula *, Svetozar Musić

Division of Materials Chemistry, Ruđer Bošković Institute, P.O. Box 180, HR-10002 Zagreb, Croatia

Abstract

The effects of Cu-dopant on the precipitation of α-FeOOH and α-Fe$_2$O$_3$ particles in highly alkaline media were investigated using ^{57}Fe Mössbauer and Fourier transform infrared (FT-IR) spectroscopies and thermal field emission scanning electron microscopy (FE SEM). Only α-(Fe, Cu)OOH solid solutions were obtained between $r = 0.0099$ and 0.0291, where $r = [Cu]/([Cu] + [Fe])$. A mixture of α-(Fe, Cu)OOH and α-(Fe, Cu)$_2$O$_3$ solid solutions was obtained between $r = 0.0385$ and 0.0566, whereas only an α-(Fe, Cu)$_2$O$_3$ solid solution was obtained between $r = 0.0698$ and 0.1666. Cu-substitutions in α-(Fe, Cu)OOH and α-(Fe, Cu)$_2$O$_3$ decreased the hyperfine magnetic field $\langle B_{hf} \rangle$ values. With increased Cu-substitution in an α-FeOOH type structure the IR shifts were observed. With an increased r value of initial solution a gradual elongation of α-(Fe, Cu)OOH particles along the crystallographic c-axis was observed. At $r = 0.0476$, some α-(Fe, Cu)OOH particles were $\sim$700 nm long, and correspondingly the width and thickness of these particles decreased markedly. With a further increase in r the length of α-(Fe, Cu)OOH particles decreased. α-(Fe, Cu)$_2$O$_3$ particles showed varying sizes in dependence on the precipitation conditions, whereas their geometrical shapes matched those typical of α-Fe$_2$O$_3$.
© 2006 Elsevier B.V. All rights reserved.

1. Introduction

The influence of various metal cations on the precipitation of α-FeOOH (goethite) and α-Fe$_2$O$_3$ (hematite) has been extensively investigated due to the importance of these compounds in nature. α-FeOOH and α-Fe$_2$O$_3$ are widely spread in nature, for example in soils, sediments and aquatic systems. Ore deposits of α-FeOOH and α-Fe$_2$O$_3$ are used in the production of raw iron. In some cases the substituted metal cations can be present in the concentrations which are of commercial interest for their extraction. The substitution of Al^{3+} for Fe^{3+} ions is particularly important in soil processes which influence adsorption/desorption processes, as well as the phase transformations of *iron oxides* (group name for iron-oxyhydroxides and -oxides).

α-FeOOH and α-Fe$_2$O$_3$ are characterized by specific colloid and surface properties, which makes these compounds very important from the academic point of view. They are often used as model systems in fundamental studies of the adsorption/desorption phenomena as well as in the investigation of the effects of metal cation incorporation in the crystal structures.

In the present work, we have focused on the influence of Cu-dopant on the properties of α-FeOOH and α-Fe$_2$O$_3$ particles precipitated in highly alkaline media. This subject was investigated by Inouye et al. [1]. They precipitated Fe^{3+} ions from mixed Fe$_2$(SO$_4$)$_3$–CuSO$_4$ solutions containing up to 5% Cu by adding KOH solution and left the suspensions to stand for different times at 30 °C. It was reported that at 2.5% Cu the formation of α-FeOOH was completely suppressed. They also tried to correlate their results with the role of small amounts of Cu in the protection of weathering steel. Cornell and Giovanoli [2] also precipitated Fe^{3+} ions in the presence of Cu^{2+} ions by adding KOH solutions at

* Corresponding author.
  E-mail address: krehul@irb.hr (S. Krehula).

pH 11–12.8. These suspensions were aged at 70 °C. Chemical analysis and XRD showed that at 9 mol% Cu only an α-Fe_2O_3 type structure was present. Martinez and McBride [3] investigated the influence of Cd^{2+}, Cu^{2+}, Pb^{2+} and Zn^{2+} ions on the transformation of ferrihydrite coprecipitates obtained at pH between 5 and 6 and found that upon the thermal treatment of coprecipitates the solubility of Cd^{2+} and Zn^{2+} ions was reduced, whereas Pb^{2+} was almost removed from the coprecipitate. On the other hand, Cu^{2+} ions were the most stable and this was explained by their structural incorporation into the host matrix. Jang et al. [4] investigated by Mössbauer spectroscopy the effects of Zn^{2+}, Cu^{2+}, Mn^{2+}, Fe^{2+}, NO_3^- or SO_4^{2-} ions on the phase transformation of hydrous ferric oxide (HFO). No transformation to hematite was observed at pH 6.5 and 65 °C in the presence of Cu^{2+} ions, whereas ageing of HFO with Cu^{2+} and Fe^{2+} ions at pH 8.5 and room temperature yielded

goethite and substoichiometric magnetite ($Fe_{3-x}O_4$). Morales et al. [5] found that in the presence of SO_4^{2-} and NO_3^- ions the formation of α-FeOOH was favoured.

All cited works were performed under very different experimental conditions and for that reason it is difficult to compare the results obtained. The aim of the present work has been to investigate: (a) the influence of Cu^{2+} concentration on the formation of α-FeOOH and α-Fe_2O_3 particles in highly alkaline media, (b) the formation of solid solutions α-(Fe, Cu)OOH and α-(Fe, Cu)$_2O_3$, and (c) the effect of Cu^{2+} ions on the size and geometrical shape of the precipitated particles. We used Mössbauer and FT-IR spectroscopies to investigate the incorporation of Cu^{2+} ions into α-FeOOH and α-Fe_2O_3 crystal structures, whereas FE SEM and EDS techniques were used to inspect the size and geometrical shape of the particles precipitated, as well as their chemical composition.

Table 1
Experimental conditions for the synthesis of samples G and BG1–BG9

Sample	Vol. 2 M FeCl$_3$ (ml)	[FeCl$_3$] (mol dm^{-3})	Vol. 0.1 M Cu(NO$_3$)$_2$ (ml)	Vol. 0.01 M Cu(NO$_3$)$_2$ (ml)	[Cu(NO$_3$)$_2$] (mol dm^{-3})	$r = $[Cu]/ ([Cu] + [Fe])	Vol. 25% w/w TMAH (ml)	Vol. H$_2$O (ml)
G	2	0.1	–	–	0	0	10	28
BG1	2	0.1	–	4	0.001	0.0099	10	24
BG2	2	0.1	–	8	0.002	0.0196	10	20
BG3	2	0.1	–	12	0.003	0.0291	10	16
BG4	2	0.1	–	16	0.004	0.0385	10	12
BG5	2	0.1	2	–	0.005	0.0476	10	26
BG6	2	0.1	2	4	0.006	0.0566	10	22
BG7	2	0.1	3	–	0.0075	0.0698	10	25
BG8	2	0.1	4	–	0.010	0.0909	10	24
BG9[a]	2	0.1	8	–	0.020	0.1666	10	20

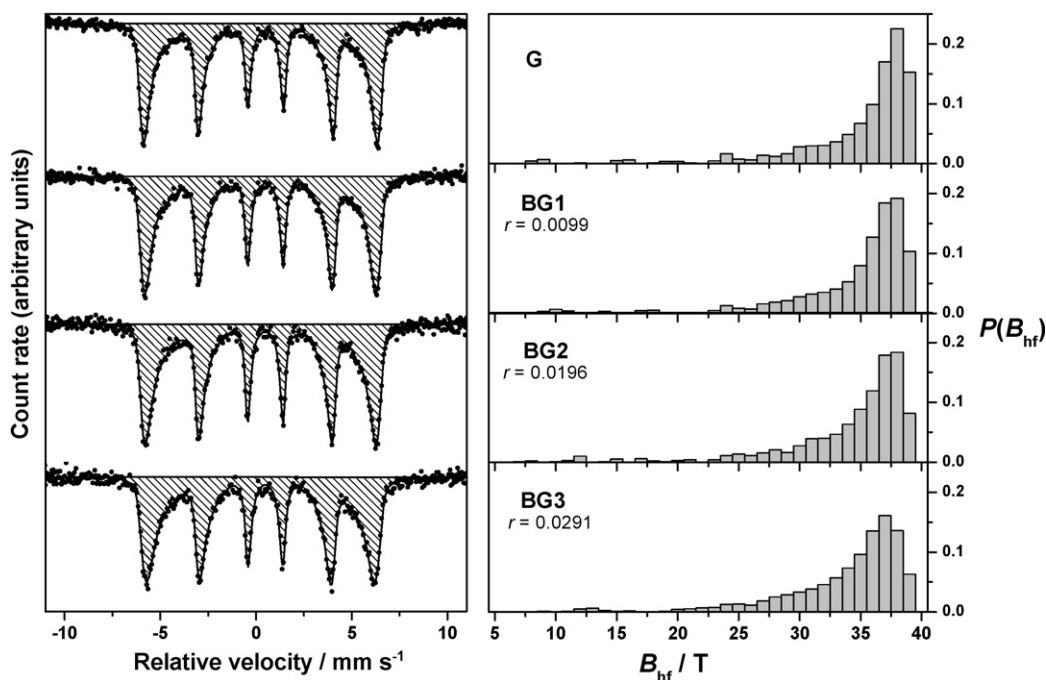[a] Reaction was not complete after 2 h of ageing; sample was obtained after 24 h of ageing.

Fig. 1. ^{57}Fe Mössbauer spectra of reference sample G and samples BG1–BG3, recorded at RT, with corresponding hyperfine magnetic field distributions.

2. Experimental

2.1. Preparation of samples

Chemicals of analytical purity, $FeCl_3 \cdot 6H_2O$ and $Cu(NO_3)_2 \cdot 3H_2O$, supplied by *Kemika*, were used. A tetra-methylammonium hydroxide (TMAH) solution (25% w/w, electronic grade 99.9999%) supplied by *Alfa Aesar*®

was used. Twice-distilled water prepared in our own laboratory was used in all experiments. Predetermined volumes of $FeCl_3$ and $Cu(NO_3)_2$ solutions and twice-distilled water were mixed, then TMAH was added as a precipitating agent. Table 1 gives exact experimental data for the preparation of samples. Thus formed aqueous suspensions were vigorously shaken for ~10 min, then heated at 160 °C, using the Parr general-purpose bomb (model 4744),
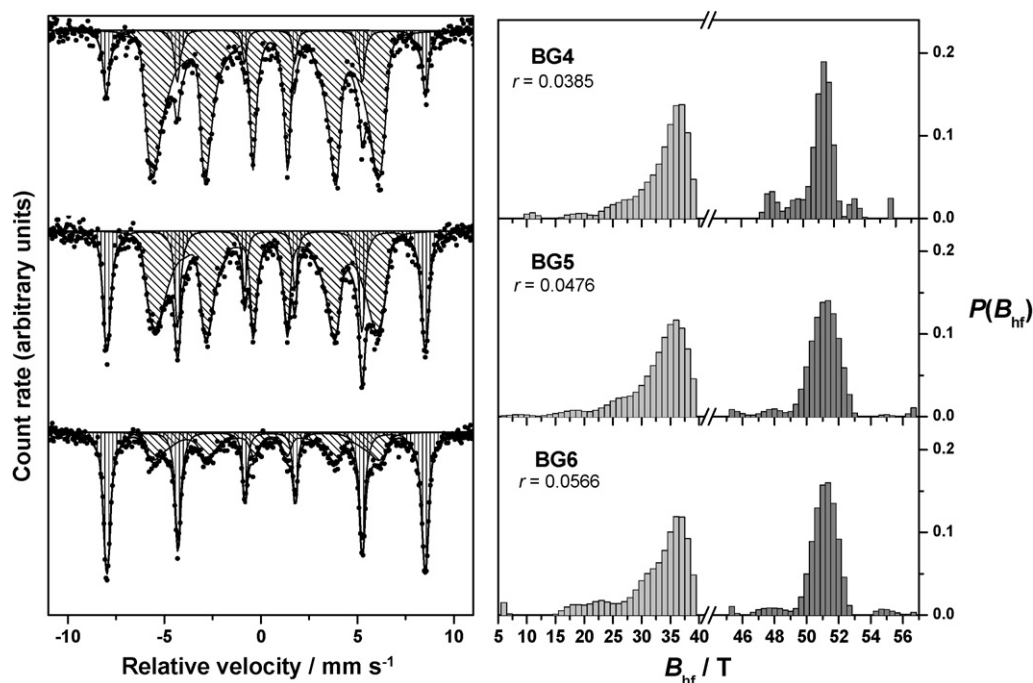

Fig. 2. ^{57}Fe Mössbauer spectra of samples BG4–BG6, recorded at RT, with corresponding hyperfine magnetic field distributions for α-FeOOH and α-Fe$_2$O$_3$.
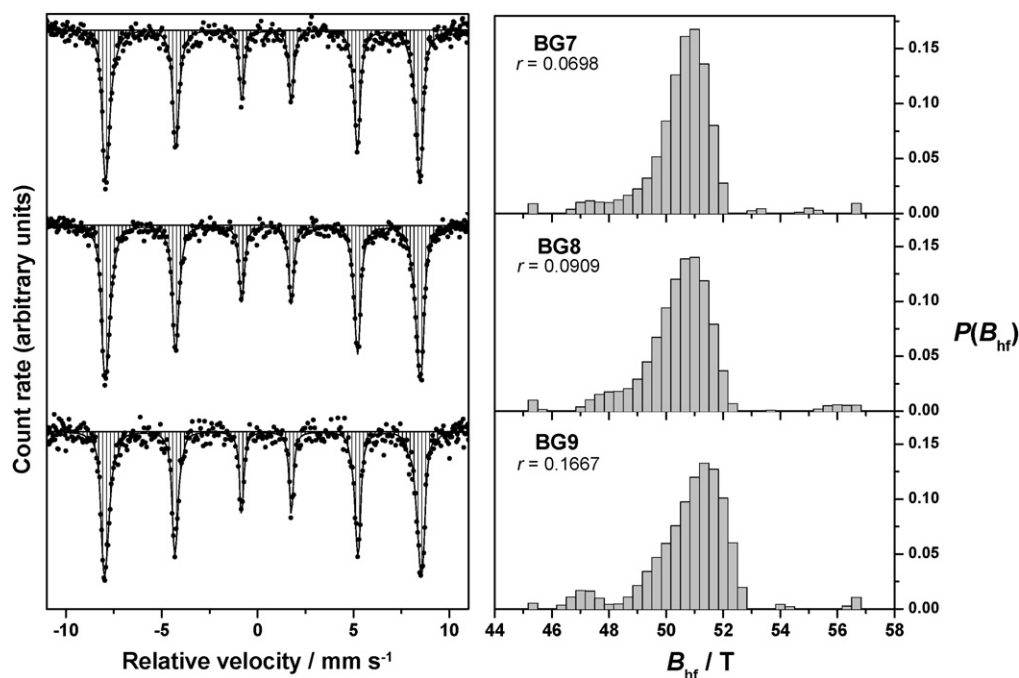

Fig. 3. ^{57}Fe Mössbauer spectra of samples BG7–BG9, recorded at RT, with corresponding hyperfine magnetic field distributions for α-Fe$_2$O$_3$.
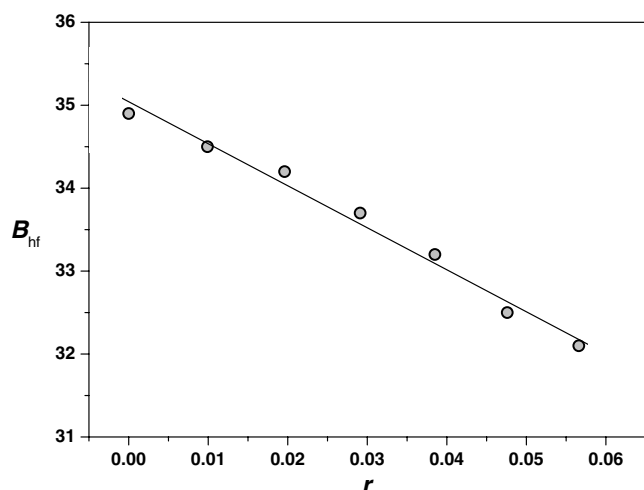
Fig. 4. Dependence of the average hyperfine magnetic field in α-FeOOH on the [Cu]/([Cu] + [Fe]) ratio (r).

comprising a Teflon vessel and a cup. After 2 h (24 h for sample BG9) of heating the precipitates were cooled to RT (mother liquor pH ~13.5–13.8) and subsequently washed with twice-distilled water to remove "neutral electrolyte". The ultraspeed *Sorvall* RC2-B centrifuge was used. After drying, all precipitates were characterized by Mössbauer and FT-IR spectroscopies, as well as high-resolution scanning electron microscopy. The concentrations of iron and copper in the particles were determined by EDS analysis.

2.2. Instrumentation

^{57}Fe Mössbauer spectra were recorded in the transmission mode using a standard *WissEl* (Starnberg, Germany) instrumental configuration. A ^{57}Co/Rh Mössbauer source was used. The velocity scale and all data refer to the metallic α-Fe absorber at RT. A quantitative analysis of the recorded spectra was made using the *MossWinn* program.

Fourier transform infrared (FT-IR) spectra were recorded at RT using a *Perkin-Elmer* spectrometer (model 2000).

The FT-IR spectrometer was linked to a PC with an installed IRDM (IR data manager) program to process the recorded spectra. The specimens were pressed into small discs using a spectroscopically pure KBr matrix.

A thermal field emission scanning electron microscope (FE SEM, model JSM-7000F, manufactured by *JEOL Ltd.*) was used. FE SEM was linked to the EDS/INCA 350 (energy dispersive X-ray analyser) manufactured by *Oxford Instruments Ltd.* The specimens were not coated with an electrically conductive surface layer.

3. Results and discussion

3.1. ^{57}Fe Mössbauer spectroscopy

The results of Mössbauer measurements are summarized in Figs. 1–4. The Mössbauer spectrum of the initial α-FeOOH (reference sample G) is shown in Fig. 1, and the corresponding ^{57}Fe Mössbauer parameters are given in Table 2. Fig. 1 shows a broadening of spectral lines with an increase in r value. Their intensities deviate from the theoretical intensity ratio 3:2:1:1:2:3. These spectra were fitted using a hyperfine magnetic field (HMF) distribution. Size and crystallinity influence the Mössbauer spectrum of α-FeOOH, so, it may vary from a well-shaped sextet to a paramagnetic doublet [6]. α-FeOOH particles smaller than ~15–20 nm show a superparamagnetic type of the Mössbauer spectrum at RT, whereas the particles smaller than 8 nm show a superparamagnetic type of the Mössbauer spectrum down to 77 K. The incorporation of metal cations into the α-FeOOH crystal structure reduces the average HMF ($\langle B_{hf} \rangle$) and influences other properties of α-FeOOH particles. These effects strongly depend on the nature of the incorporated metal cation. Murad and Schwertmann [7] investigated a possible combined effect of poor crystallinity and metal cation substitution on the Mössbauer spectra of α-FeOOH. In the present case the effect of poor crystallinity of α-FeOOH can be neglected and a decrease in $\langle B_{hf} \rangle$ can be assigned to the effect of Cu-substitution into the α-FeOOH structure. In this study,

Table 2
^{57}Fe Mössbauer parameters calculated for samples G and BG1–BG9 and identification

Sample	Spectral line	δ (mm s^{-1})	E_q or Δ (mm s^{-1})	B_{hf} (T)	Γ (mm s^{-1})	Area (%)	Identification
G	M	0.37	− 0.26	34.9	0.28	100	α-FeOOH
BG1	M	0.36	− 0.26	34.5	0.27	100	α-(Fe, Cu)OOH
BG2	M	0.37	− 0.25	34.2	0.25	100	α-(Fe, Cu)OOH
BG3	M	0.37	− 0.25	33.8	0.28	100	α-(Fe, Cu)OOH
BG4	M$_1$	0.37	− 0.24	33.2	0.27	84.2	α-(Fe, Cu)OOH
	M$_2$	0.36	− 0.19	51.1	0.24	15.8	α-(Fe, Cu)$_2$O$_3$
BG5	M$_1$	0.38	− 0.22	32.5	0.28	67.7	α-(Fe, Cu)OOH
	M$_2$	0.37	− 0.19	51.0	0.26	32.3	α-(Fe, Cu)$_2$O$_3$
BG6	M$_1$	0.38	− 0.22	32.1	0.41	36.8	α-(Fe, Cu)OOH
	M$_2$	0.38	− 0.21	51.0	0.27	63.2	α-(Fe, Cu)$_2$O$_3$
BG7	M	0.37	− 0.20	50.6	0.29	100	α-(Fe, Cu)$_2$O$_3$
BG8	M	0.37	− 0.19	50.7	0.30	100	α-(Fe, Cu)$_2$O$_3$
BG9	M	0.38	− 0.18	50.8	0.24	100	α-(Fe, Cu)$_2$O$_3$

Errors, $\delta = \pm 0.01$ mm s^{-1}; $E_q = \pm 0.01$ mm s^{-1}; $B_{hf} = \pm 0.2$ T. Isomer shift is given relative to α-Fe.

we used a reference α-FeOOH (sample G) precipitated in the highly alkaline medium (pH $\sim$13.5–13.8) using a strong organic alkali as the precipitating agent and autoclaving thus formed suspension [8]. This precipitation method made it possible to obtain well-defined colloid α-FeOOH particles with a high degree of reproducibility. Thus it was possible to assign the observed effect to Cu-substitution in the α-FeOOH structure.

Up to $r = 0.0291$, where $r = [\text{Cu}]/([\text{Cu}] + [\text{Fe}])$ in initial solution, Mössbauer spectra (Fig. 1) showed only the presence of an α-FeOOH type structure. At the same concentration ratio $\langle B_{hf} \rangle$ decreased from 34.9 T (sample G) to 33.8 T (sample BG3). Fig. 2 shows RT Mössbauer spectra of samples BG4, BG5 and BG6 consisting of the superposition of two sextets, which can be assigned to the formation of two types of solid solutions, α-(Fe, Cu)OOH and α-(Fe, Cu)$_2$O$_3$. The $\langle B_{hf} \rangle$ value of α-(Fe, Cu)OOH further decreased to 32.1 T (sample BG6). The $\langle B_{hf} \rangle$ value of α-(Fe, Cu)$_2$O$_3$ did not change significantly (51.1–51.0 T) for samples BG4–BG6; however, this value was evidently smaller than that of reference α-Fe$_2$O$_3$ (51.8 T) [9]. Mössbauer spectra of samples BG7, BG8 and BG9 ($r = 0.0698$–0.1666) showed only one sextet (Fig. 3) and $\langle B_{hf} \rangle$ values of 50.6, 50.7 and 50.8 T, respectively, were measured. It can be noted here that in the case of sample BG9 there was no significant precipitation after 2 h of autoclaving; thus the precipitate was collected after 24 h of autoclaving. In Figs. 1–3 the corresponding hyperfine field distributions for α-(Fe, Cu)OOH and α-(Fe, Cu)$_2$O$_3$ are also shown. Fig. 4 shows a linear decrease of $\langle B_{hf} \rangle$

measured for α-(Fe, Cu)OOH with an increased concentration ratio r in initial solution. These measurements showed high capabilities of Mössbauer spectroscopy to investigate the incorporation of Cu^{2+} cations into the α-FeOOH and α-Fe$_2$O$_3$ crystal structures. Furthermore, Mössbauer spectroscopy is more sensitive and accurate than X-ray diffraction in the determination of mixed α-FeOOH and α-Fe$_2$O$_3$ phases in the precipitates. Specifically, this is pronounced if the fraction of α-FeOOH is significantly higher than that of α-Fe$_2$O$_3$, and vice versa [10].
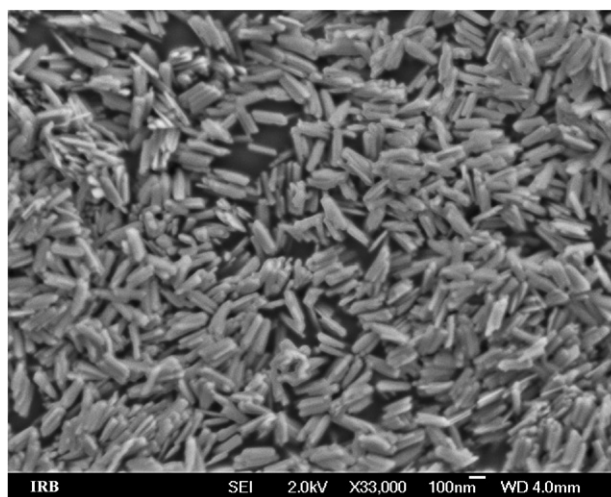

Fig. 6. FE SEM micrograph of reference α-FeOOH (sample G).
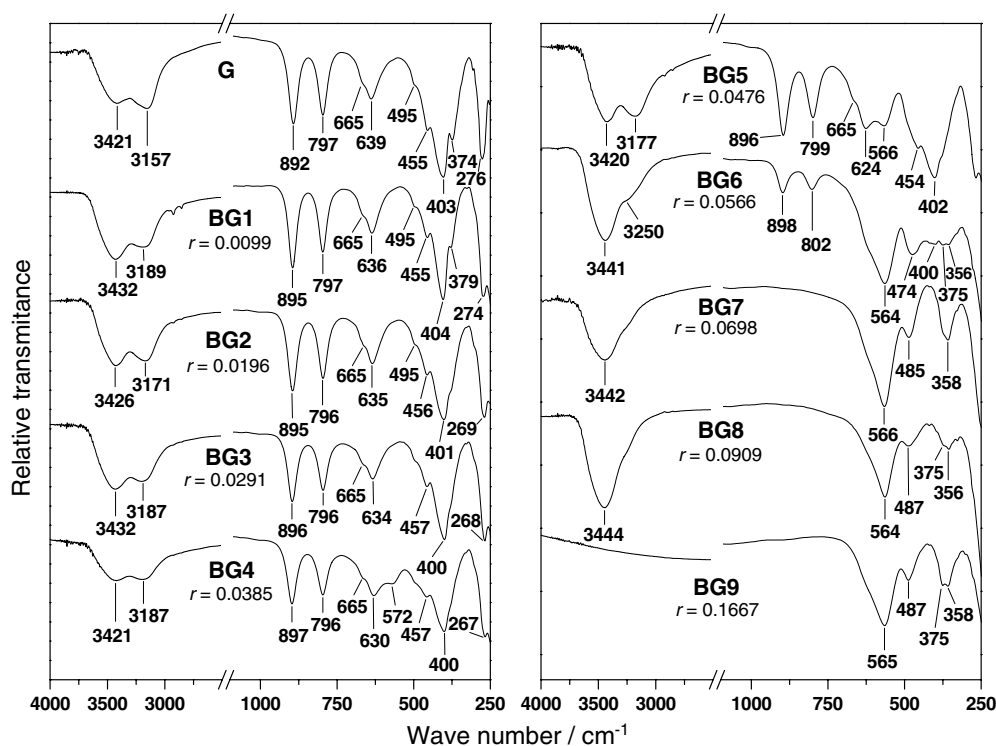

Fig. 5. FT-IR spectra of sample G and samples BG1–BG9 recorded at RT.

Generally, the incorporation of metal cations with charges other than three into the crystal structures of α-FeOOH and α-Fe_2O_3 will change electrical neutrality in a crystal lattice. Counter charge will be required to restore electrical neutrality. In the case of the formation of solid solutions of Zn^{2+} ions and α-Fe_2O_3 this charge balance was achieved by oxygen vacancies [11]. It was also suggested [12] that Sn^{4+}, Ti^{4+} and Mg^{2+} may occupy both the interstitial and substitutional sites in an α-Fe_2O_3 related structure. Carvalho-e-Silva et al. [13] suggested that the Ni^{2+} for Fe^{3+} substitution in α-FeOOH can be explained by a mechanism that includes the compensation for the charge imbalance in a crystal lattice. In accordance with this model the Ni^{2+} for Fe^{3+} substitution is accompanied by a proton capture resulting in $NiO_2(OH)_4$ octahedra. In the case of Cu^{2+} ions in the α-FeOOH crystal lattice
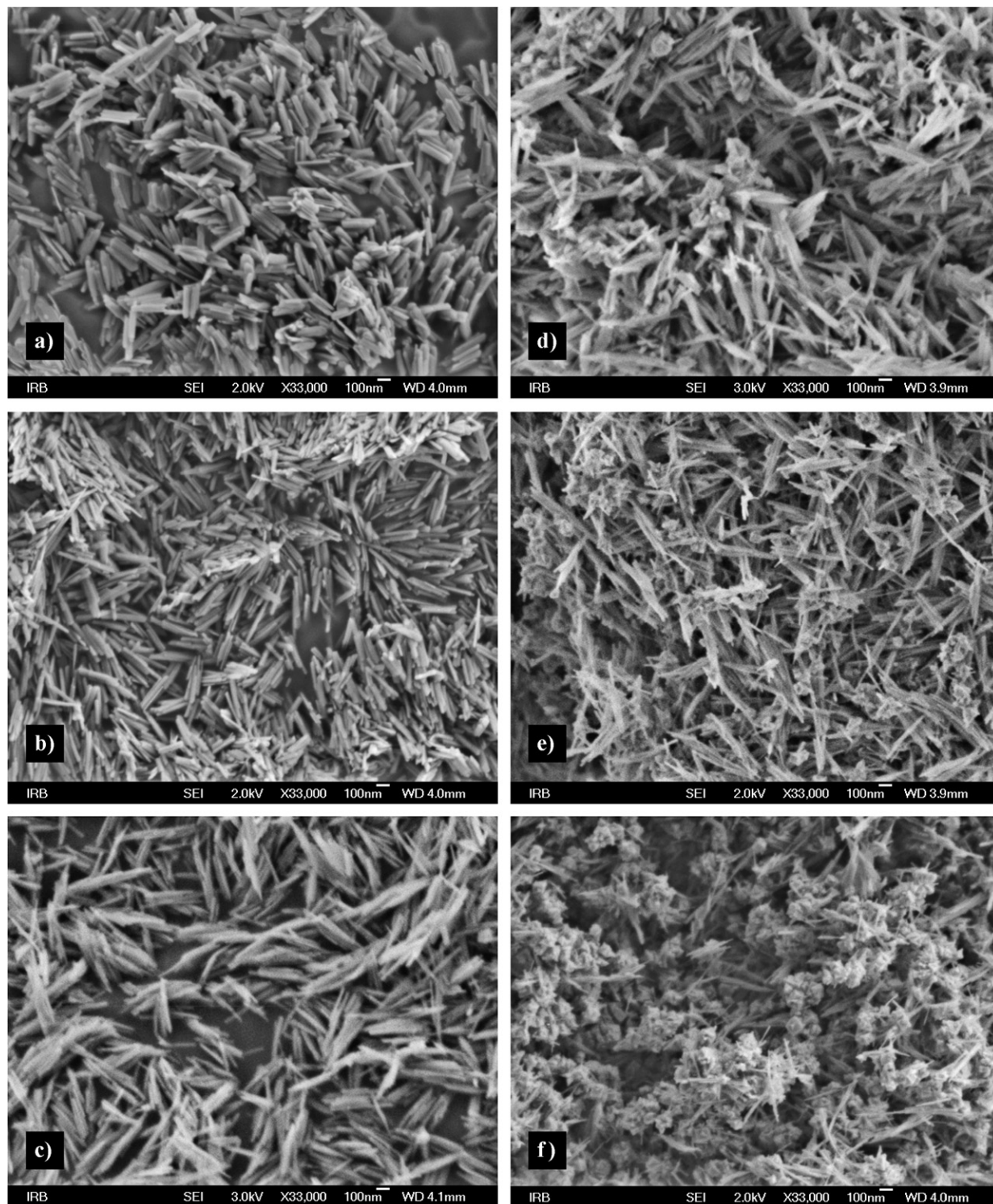

Fig. 7. FE SEM micrographs of samples: (a) BG1, (b) BG2, (c) BG3, (d) BG4, (e) BG5 and (f) BG6.

there is a possibility of: (a) proton capture to compensate for the electric charge in this crystal structure or (b) mixed effect which includes proton capture, as well as counter charge of crystal defects in the form of oxygen vacancies.

3.2. FT-IR spectroscopy

Fig. 5 shows the characteristic parts of the FT-IR spectra of sample G and samples BG1–BG9. The corresponding r values are also denoted. The FT-IR spectrum of sample G corresponds to a pure α-FeOOH. At high wave numbers the spectrum showed two IR bands at 3421 and 3157 cm^{-1} which can be assigned to the stretching vibrations of adsorbed H_2O molecules and structural OH^- groups, respectively. Sample G is characterized by two very intensive IR bands at 892 and 797 cm^{-1} which can be assigned to Fe–O–H bending vibrations. Verdonck et al. [14] compared experimental data and calculated vibrational frequencies of α-FeOOH and α-FeOOD. They found that the IR bands at 630, 495 and 270 cm^{-1} were rather insensitive to deuteration, hence those vibrations were assigned to the Fe–O stretching. Cambier [15] reported that an intense IR band at about 630 cm^{-1} was influenced by the geometrical shape of α-FeOOH particles. The incorporation of Cu^{2+} ions into the α-FeOOH structure influences the corresponding FT-IR spectra. For example, the IR bands at 892 and 797 cm^{-1} observed in pure α-FeOOH (sample G) were shifted to 898 and 802 cm^{-1} in sample BG6 ($r = 0.0566$). Moreover, the IR band at 639 cm^{-1} was shifted to 624 cm^{-1} in sample BG5 ($r = 0.0476$). Sample BG6 also showed a very intensive IR band at 564 cm^{-1} and a band at 474 cm^{-1} which can be assigned to the α-Fe_2O_3 type structure or, more precisely, in the present case to the α-$(Fe, Cu)_2O_3$ solid solution. The IR band at 564 cm^{-1} practically did not change its position; however, the IR band at 474 cm^{-1} shifted to 487 cm^{-1}. Iglesias and Serna [16] reported the IR spectra of α-Fe_2O_3 particles of different geometrical shapes. α-Fe_2O_3 spheres showed IR bands at 575, 485, 385 and 360 cm^{-1}, whereas α-Fe_2O_3 laths showed IR bands at 650, 525, 440 and 300 cm^{-1}.

3.3. FE SEM

Fig. 6 shows an FE SEM micrograph of reference α-FeOOH particles prepared in the course of an earlier work [8], whereas Fig. 7 shows FE SEM micrographs of
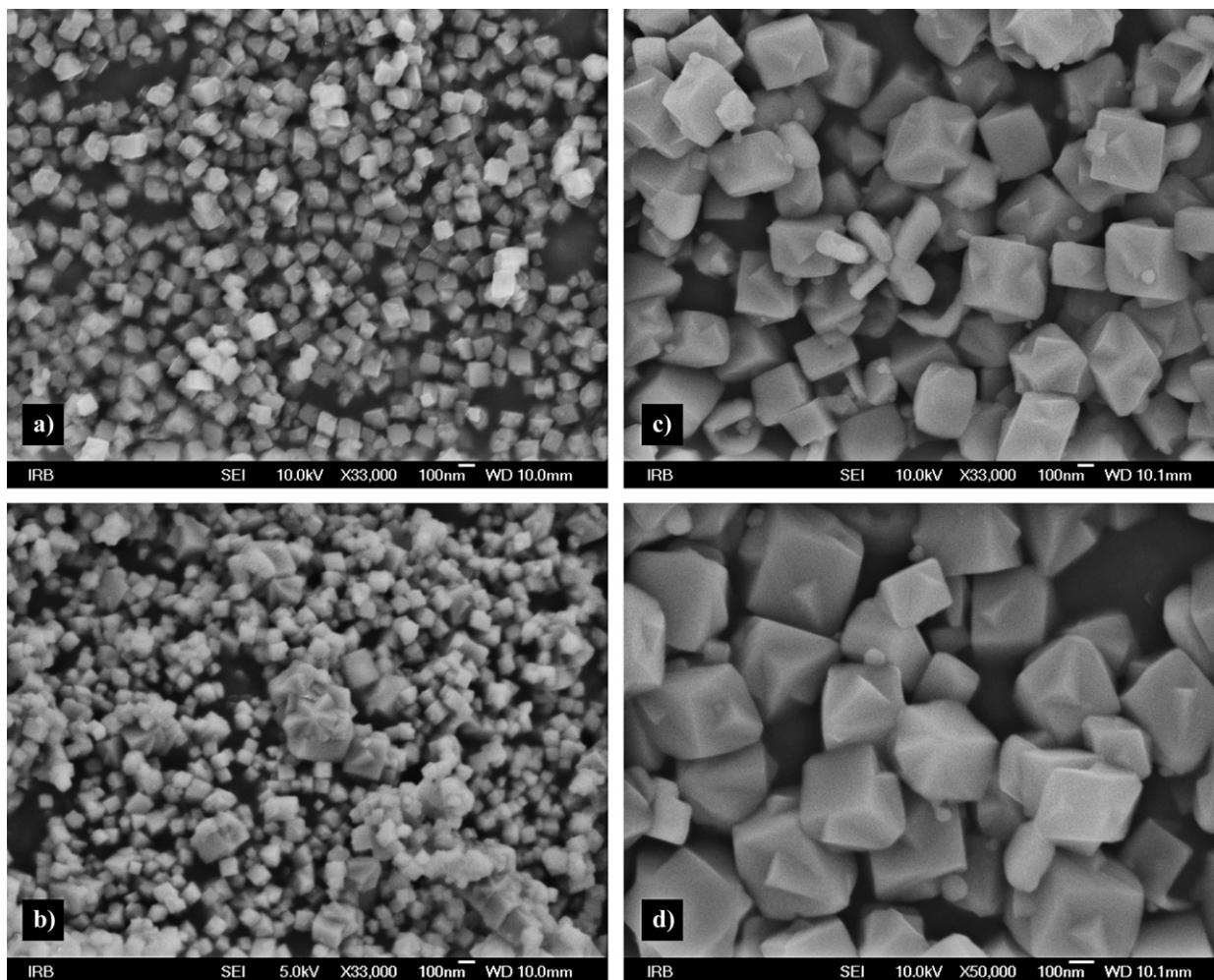

Fig. 8. FE SEM micrographs of samples: (a) BG7, (b) BG8, (c) and (d) BG9.

samples BG1–BG6. The particles of sample BG1 are ~250–300 nm in size. With an increase in Cu-substitution, an elongation of α-FeOOH particles occurs, which is in line with the corresponding anisotropy of α-FeOOH crystallites along the *c*-axis. Sample BG5 showed the most elongated α-(Fe, Cu)OOH particles, some of them up to ~700 nm long. Also, with increased *r* value a gradual decrease in width (*b*-axis direction) and thickness (*a*-axis direction) was observed. This effect was most pronounced in sample BG5. However, in sample BG6 the length of α-(Fe, Cu)OOH particles decreased.

Fig. 8 shows FE SEM micrographs of samples BG7, BG8 and BG9 (two details). Sample BG7 micrograph (Fig. 8a) shows the α-(Fe, Cu)$_2$O$_3$ particles of good uniformity. On the other hand, the formation of α-(Fe, Cu)$_2$O$_3$ aggregates and a certain fraction of much bigger α-(Fe, Cu)$_2$O$_3$ particles were visible in sample BG8 micrograph (Fig. 8b). Sample BG9 micrographs (Fig. 8c and d) show much bigger α-(Fe, Cu)$_2$O$_3$ particles of a more articulate geometry than that in the samples BG7 and BG8. However; it should be noted that the crystallization of sample BG9 took longer (24 h) than was the case with other samples (2 h). Taking into account the experimental conditions and FE SEM micrographs containing the α-(Fe, Cu)$_2$O$_3$ phase, the Mössbauer parameters measured for the corresponding samples can be better understood.

4. Conclusion

- Acicular and monodisperse α-FeOOH particles, prepared in the course of an earlier work [8], were used as a reference material in the investigations of Cu-doping on the properties of α-FeOOH and α-Fe$_2$O$_3$.
- The $\langle B_{hf} \rangle$ value of the hyperfine magnetic field was shown as the Mössbauer parameter sensitive to Cu-doping of α-FeOOH. The formation of merely α-(Fe, Cu)OOH solid solutions was observed up to $r = 0.0291$, the mixture of α-(Fe, Cu)OOH and α-(Fe, Cu)$_2$O$_3$ solid solutions was obtained between $r = 0.0385$ and 0.0566, whereas only an α-(Fe, Cu)$_2$O$_3$ solid solution was found between $r = 0.0698$ and 0.1666.
- FT-IR spectra showed certain changes upon the incorporation of Cu^{2+} ions into the α-FeOOH structure. The IR bands at 892 and 797 cm^{-1} observed in the reference α-FeOOH sample were shifted to 898 and 892 cm^{-1} at $r = 0.0566$, whereas the IR band at 639 cm^{-1} was shifted to 624 cm^{-1} at $r = 0.0476$. The FT-IR spectra of the samples with *r* between 0.0698 and 0.1667 showed the main features characteristic of an α-Fe$_2$O$_3$ type structure. FT-IR spectroscopy can be used rather as a qualitative technique in studying the precipitation of α-FeOOH and α-Fe$_2$O$_3$ particles.

- Cu-substitutions brought into the α-FeOOH crystal structure led to an increase in its anisotropy along the *c*-axis. Accordingly, with an increased *r* value an elongation of α-(Fe, Cu)OOH particles was observed. The length of α-(Fe, Cu)OOH particles increased from ~250–300 nm at $r = 0.0099$ up to ~700 nm for some particles precipitated at $r = 0.0476$.

- At *r* between 0.0698 and 0.1666 the α-(Fe, Cu)$_2$O$_3$ particles with characteristic geometrical shapes were obtained. Their differences in size and geometrical shapes were a direct consequence of the precipitation procedure.

References

[1] K. Inouye, S. Ishii, K. Kaneko, T. Ishikawa, Z. Anorg. Allg. Chem. 391 (1972) 86.
[2] R.M. Cornell, R. Giovanoli, Polyhedron 7 (1988) 385.
[3] C.E. Martinez, M.B. McBride, Clay Clay Miner. 46 (1998) 537.
[4] J.-H. Jang, B.A. Dempsey, G.L. Catchen, W.D. Burgos, Coll. Surf. A: Physicochem. Eng. Aspects 221 (2003) 55.
[5] A.L. Morales, C.A. Barrero, F. Jaramillo, C. Arroyave, J.-M. Greneche, Hyperfine Interact. 148/149 (2003) 135.
[6] E. Murad, J.H. Johnston, in: G.J. Long (Ed.), Iron Oxides and Oxyhydroxides in Mössbauer Spectroscopy Applied to Inorganic Chemistry, vol. 2, Plenum Publishing Corporation, New York, 1987, pp. 507–582.
[7] E. Murad, U. Schwertmann, Clay Miner. 18 (1983) 301.
[8] S. Krehula, S. Popović, S. Musić, Mater. Lett. 54 (2002) 108.
[9] S. Musić, I. Czakó-Nagy, S. Popović, A. Vértes, M. Tonković, Croat. Chem. Acta 59 (1986) 833.
[10] S. Musić, S. Popović, J. Radioanal. Nucl. Chem. 111 (1987) 27.
[11] I. Ayub, F.J. Berry, R.L. Bilsborrow, Ö. Helgason, R.C. Mercader, E.A. Moore, S.J. Stewart, P.G. Wynn, J. Solid State Chem. 156 (2001) 408.
[12] F.J. Berry, C. Greaves, Ö. Helgason, J. McManus, H.M. Palmer, R.T. Williams, J. Solid State Chem. 151 (2000) 157.
[13] M.L. Carvalho-e-Silva, A.Y. Ramos, H.C.N. Tolentino, J. Enzweiler, S.M. Netto, M. Do Carmo Martins Alves, Am. Mineral. 88 (2003) 876.
[14] L. Verdonck, S. Hoste, F.F. Roelandt, G.P. Van der Kelen, J. Mol. Struct. 79 (1982) 273.
[15] P. Cambier, Clay Miner. 21 (1986) 191.
[16] J.E. Iglesias, C.J. Serna, Miner. Petrogr. Acta 29A (1985) 363–370.